The Reactivity of Heme in Biological Systems: Autocatalytic Formation of Both Tyrosine−Heme and Tryptophan−Heme Covalent Links in a Single Protein Architecture†

Zoi Pipirou,‡ Andrew R. Bottrill,§ Dimitri A. Svistunenko,|| Igor Efimov,‡ Jaswir Basran,⊥ Sharad C. Mistry,§ Christopher E. Cooper,|| and Emma Lloyd Raven*,‡

Department of Chemistry, Henry Wellcome Building, University of Leicester, University Road, Leicester, LE1 7RH, England, Protein and Nucleic Acid Chemistry Laboratory, Hodgkin Building, University of Leicester, Lancaster Road, Leicester LE1 9HN, England, Department of Biochemistry, Henry Wellcome Building, University of Leicester, Lancaster Road, Leicester, LE1 9HN, England, and Department of Biological Sciences, University of Essex, Wivenhoe Park, Colchester, CO4 3SQ, England

Received August 1, 2007; Revised Manuscript Received September 13, 2007

ABSTRACT: We have previously shown that introduction of an engineered Met160 residue in ascorbate peroxidase (S160M variant) leads to the formation of a covalent link between Met160 and the heme vinyl group [Metcalfe, C. L., et al. (2004) *J. Am. Chem. Soc. 126,* 16242−16248]. In this work, we have used electronic spectroscopy, HPLC, and mass spectrometry to show that the introduction of a tyrosine residue at the same position (S160Y variant) leads, similarly, to the formation of a heme−tyrosine covalent link in an autocatalytic reaction that also leads to formation of a second covalent link from the heme to Trp41 [Pipirou, Z., et al. (2007) *Biochemistry 46,* 2174−2180]. Stopped-flow and EPR data implicate the involvement of a tyrosyl radical in the reaction mechanism. The results indicate that the heme can support the formation of different types of covalent links under appropriate conditions. The generality of this idea is discussed in the context of other heme enzymes.

The heme prosthetic group is used commonly in biology. It is usually found associated with proteins as a noncovalent complex, for example in the globins and the *b*-type cytochromes. There are examples, however, in which the heme is bound to the protein through a covalent link to one or more amino acids. The cytochromes *c* (*1*) are probably the most well-known example of this: in this case, one or both of the heme vinyl groups are bound to the protein through thioether bonds to cysteine residues. Recently, however, it has become clear that the presence of a covalently bound heme group is not a special privilege of the cytochromes *c*. For example, the mammalian peroxidase enzymes are known to contain sulfonium links between the heme 2-vinyl group and a Met residue (in myeloperoxidase) and/or two ester links between heme methyl groups and Glu/Asp residues (in myeloperoxidase, lactoperoxidase) (*2*−*5*). Other examples include the CYP4 family of cytochrome P450s which contain a similar ester link between the heme methyl group and a Glu residue (*2*, *6*, *7*); a cyanobacterial hemoglobin, which contains a covalent link between the vinyl group and a His residue (*8*); and the heme chaperone CcmE which uses a different vinyl−His covalent link (*9*, *10*).

Recently, various studies from a number of laboratories have shown that the formation of covalent links to the heme of the type described above are not a unique feature of these particular proteins and can actually be engineered into an existing heme protein framework if an appropriate residue is introduced at an appropriate location and if the correct metal oxidation states are accessible (*11*−*16*). Collectively, these data have led to an emerging view that the existence of a specific covalent link is largely dictated by structural geometry and, in the catalytic enzymes, heme reactivity. This represents a substantial departure in the way we think about these modified heme groups because it tells us that the strategic positioning of a suitable amino acid within close proximity of the heme group, and contained within a structurally competent protein architecture, is all that is needed for a covalent link from the heme to the protein to form. By implication, this leads one to conclude that "activation" of the heme substituents is accessible in numerous heme protein architectures and is dictated by the iron chemistry and the structural environment. It follows logically that some proteins might actually need to be poised in an environment that controls the inherent reactivity of the heme group by specifically "switching off" the machinery required for formation of these covalent links. As a case in point, we have noted (*17*) that a covalent link between the heme and an engineered Met residue, analogous to that found in the mammalian peroxidases, can be incorporated into the ascorbate peroxidase framework but that cytochrome *c* peroxidase, which already contains a Met residue at this position (Met172), does not form the same covalent heme−Met link under any accessible conditions.

† This work was supported by grants from The Leverhulme Trust, BBSRC (Grants BB/C00602X/1 and IIP0206/009) and EPSRC (studentship to Z.P.).

* To whom correspondence should be addressed. Tel: +44 (0)116 2297047. Fax: +44 (0)116 252 2789. E-mail: emma.raven@le.ac.uk.

‡ Department of Chemistry, University of Leicester.

§ Protein and Nucleic Acid Chemistry Laboratory, University of Leicester.

|| Department of Biological Sciences, University of Essex.

⊥ Department of Biochemistry, University of Leicester.

10.1021/bi7015316 CCC: $37.00
Published on Web 10/25/2007

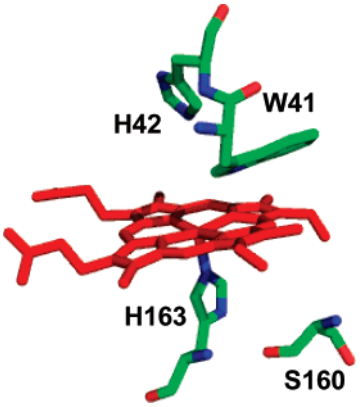

FIGURE 1: The active site of rsAPX.

If it is the case that the heme group *per se* is inherently reactive and its reactivity is controlled by the iron and the protein hardware, then it follows that the heme should, in principle, react with *any* nucleophilic amino acid, not just those observed so far in biological systems. In this work, we have tested the generality of this hypothesis by the introduction of a Tyr residue (S160Y variant, Figure 1) into ascorbate peroxidase at a position that has been shown (*11*) to allow formation of a methionine−heme covalent link (S160M variant) through a H_2O_2-dependent activation process. We find that Tyr160 does indeed form a covalent link to the heme in an autocatalytic reaction that also leads to formation of a second covalent link to Trp41. We find that the formation of these links has a profound effect on the redox properties of the heme iron. The implications of these data in terms of current understanding of heme group reactivity are discussed.

EXPERIMENTAL PROCEDURES

Materials. L-Ascorbic acid (Aldrich Chemical Co.) and all buffers (Fisher) were of the highest analytical grade (99%+ purity) and used without further purification. Sinapinic acid and α-cyano-4-hydroxycinnamic acid were purchased from Fluka. All other chemicals were purchased from Sigma. Water was purified by an Elga purelab purification system, and all buffers were filtered (0.2 μm) prior to use. Hydrogen peroxide solutions were freshly prepared by dilution of a 30% (v/v) solution (BDH): exact concentrations were determined using the published absorption coefficient ($\epsilon_{240} = 39.4\ M^{-1}\ cm^{-1}$) (*18*). All molecular biology kits and enzymes were used according to manufacturer's protocols.

Mutagenesis, Protein Expression, and Purification. Site-directed mutagenesis on recombinant soybean cytosolic APX[1] (rsAPX) was performed according to the Quikchange protocol (Stratagene Ltd, Cambridge, U.K.). For the S160Y mutation, the primers were 5′-CGTTGCTCTA**TAT**GGGGGT-CACACTATTGG-3′ (forward primer) and 5′-CCAATAGT-GTGACCCCC**ATA**TAGAGCAACG-3′ (reverse primer), with the mutation shown in bold. Bacterial fermentation of cells and purification of rsAPX and S160Y were carried out according to published procedures (*11*, *19*). Purified samples of rsAPX and S160Y showed wavelength maxima at 407 (107), 525, and ≈630 nm (*20*) and 413 (134), 529, and 562 nm, respectively. Enzyme concentrations for rsAPX and S160Y were determined using absorption coefficients of $\epsilon_{407} = 107\ mM^{-1}\ cm^{-1}$ (*20*) and $\epsilon_{405} = 134\ mM^{-1}\ cm^{-1}$, respectively. Preparation of apoenzyme and reconstitution with iron (III) deuteroporphyrin IX chloride was carried out according to published procedures (*17*).

Electronic Absorption Spectroscopy. Spectra were collected using a Perkin-Elmer Lambda 35 or 40 spectrophotometer, linked to a PC workstation running UV-Winlab software. Pyridine hemochromagen assays before and after reaction of enzyme with H_2O_2 were carried out according to published protocols (*17*). The pyridine hemochromagen experiment proceeds as follows: a solution of protein is mixed with a solution of pyridine in NaOH. Oxidized pyridine hemochromagen, which is a soluble and stable compound, is formed rapidly. The spectrum between 600 and 500 nm is recorded just after addition of solid sodium dithionite, which yields the relatively unstable reduced pyridine hemochromagen. An absorbance maximum of 557 nm is expected for protoheme (*17*). The complete transfer of heme from the protein to the pyridine was assessed by determining the absorbance at maximum ($\lambda = 557$ nm) and minimum ($\lambda = 540$ nm) wavelengths; a ratio of $A_{557}/A_{540} = 3.5$ is found for protoheme.

Acidified Butanone Extraction. Acid butanone extractions were carried out as reported previously (*21*). Specifically, an aqueous solution of protein was titrated with 1 M HCl to a pH of 1.5. An equivalent volume of ice-cold 2-butanone was added with gentle but continuous stirring. After a period of cooling on ice, two distinct layers were observed. Transfer of heme to the organic layer (visualized by red color) indicates absence of covalent links between the heme and the protein, and *vice versa*.

Kinetic Measurements. Steady-state measurements (100 mM potassium phosphate, pH 7.0, 25 °C) for oxidation of ascorbate were carried out according to published protocols (*22*). Multiple wavelength absorption studies were carried out using a photodiode array detector and X-SCAN software (Applied Photophysics). Spectral deconvolution was performed by global analysis and numerical integration methods using PROKIN software (Applied Photophysics). To investigate reaction of S160Y with H_2O_2, the enzyme (20 μM in 100 mM potassium phosphate buffer, pH 7, 25.0 °C) was mixed with varying concentrations of H_2O_2 and the reaction was followed over time scales ranging from 300 ms to 4200 s.

Electron Paramagnetic Resonance. All EPR spectra were measured using a Bruker EMX EPR spectrometer (X-band) at a modulation frequency of 100 kHz. Accurate g-values were obtained using the built-in microwave frequency counter and a 2,2-diphenyl-1-picrylhydrazyl powder standard ($g = 2.0037 \pm 0.0002$ (*23*)). A spherical high quality Bruker resonator SP9703 and an Oxford Instruments liquid helium system were used to measure low-temperature EPR spectra. Spectra for blank samples (frozen water) were subtracted from the corresponding protein spectrum to eliminate the baseline caused by the resonator's walls, quartz insert, or quartz EPR tube. Individual signals were simulated using SimFonia v.1.25 (Bruker Analytische Messtechnik GmbH). The absolute free radical concentration was determined by comparison of the second integral of a pure line shape of

[1] Abbreviations: APX, ascorbate peroxidase; rsAPX, recombinant soybean cytosolic ascorbate peroxidase; HAO, hydroxylamine oxidoreductase.

the free radical EPR signal, free from the $g = 2$ components of both high-spin ferric heme and Compound I, with the signal of a 98 μM Cu^{2+} standard. For spectra of ferric rsAPX and S160Y, 250 μL of enzyme (160 μM in 100 mM potassium phosphate, pH 7) was mixed with equal volume of buffer; for spectra of rsAPX and S160Y after H_2O_2 treatment, 180 μL of enzyme solution (98 μM in 100 mM potassium phosphate, pH 7) was mixed with 40 μL of H_2O_2 solution (440 μM in 100 mM potassium phosphate, pH 7) (final concentrations = 80 μM enzyme/80 μM H_2O_2).

High Performance Liquid Chromatography. HPLC analysis of protein and peptide samples and tryptic digestion were carried out according to published protocols (*17*).

Mass Spectrometry. MALDI-TOF mass spectrometry analysis of protein and peptide samples and MS/MS analysis of peptide samples were carried out according to published protocols (*17*). Theoretical isotope patterns for heme and peptide fragments of interest were calculated by entering the desired chemical formula in the "Sheffield ChemPuter Isotope Pattern Calculator" (http://winter.group.shef.ac.uk/chemputer/isotopes.html). The results are presented with the most intense line set to 100%. Experiments on peptide isotope patterns were carried out with the assistance of the EPSRC National Mass Spectrometry Service in Swansea.

Determination of Fe^{3+}/Fe^{2+} Reduction Potential. Fe^{3+}/Fe^{2+} reduction potentials for rsAPX and S160Y were determined by simultaneous reduction with a dye of known potential (*24*) according to previous methodology (*25*). The assay contained xanthine (300 μM), xanthine oxidase (50 nM), and enzyme (3−4 μM). The buffer (100 mM potassium phosphate buffer, pH 7.0) was made oxygen free using glucose (5 mM), glucose oxidase (50 μg/mL), and catalase (5 μg/mL). For measurement of the reduction potentials of rsAPX and S160Y before reaction with H_2O_2 the reaction also contained phenosafranin ($E_{m,7} = -252$ mV) (*26*). Absorbance changes corresponding to reduction of heme were measured at the isosbestic point for phenosafranine (407 nm); reduction of the dye was measured at 520 nm where the change due to heme reduction was negligible. For measurement of the reduction potential of S160Y after reaction with H_2O_2, the same experiment was also carried out using indigo trisulfonate ($E_{m,7} = -81$ mV) as a dye (*26*). Reduction of the dye was measured at the wavelength maximum of the dye (600 nm), where the change due to heme reduction was negligible; absorbance changes corresponding to reduction of heme were measured at 440 nm, subtracting the contribution from the dye. In all cases, linear Nernst plots for one-electron reduction of heme (25 mV $\ln(E_{ox}/E_{red})$) (where E_{ox} = concentration of oxidized enzyme, E_{red} = concentration of reduced enzyme) and two-electron reduction of dye (12.5 mV $\ln(D_{ox}/D_{red})$ (where D_{ox} = concentration of oxidized dye, D_{red} = concentration of reduced dye) produced the expected slope of 1 across a wide range of potentials, and the intercept gives a reliable value for $\Delta E_{m,7}$ with an error of ±2 mV. UV−visible spectra obtained in all experiments were analyzed using SPECFIT (*27*) for singular value decomposition based on factor analysis. All potentials reported in this paper are given versus the normal hydrogen electrode (NHE).

RESULTS

Characterization of S160Y. The S160Y variant was expressed as *apo*-enzyme, which was reconstituted with hemin. This resulted in formation of a red enzyme with absorption maxima at 413, 529, and $562^{(sh)}$ nm (Figure 2a). Comparison with the corresponding spectrum of rsAPX (Figure 2a) shows that the Soret peak for S160Y is red-shifted compared to rsAPX and that there is no band at 630 nm, both of which are indicative of formation of low-spin heme in S160Y.

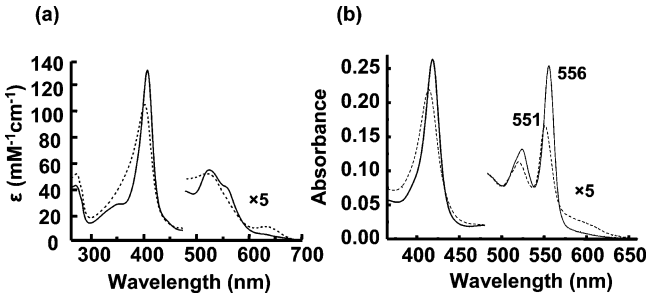

FIGURE 2: (a) Electronic absorption spectra of S160Y (solid line) and rsAPX (dashed line). The visible region has been multiplied by a factor of 5 (100 μM potassium phosphate, pH 7.0, 25.0 °C). (b) Spectra of the reduced pyridine hemochromagen complexes of S160Y before (solid line) and after (dashed line) reaction with H_2O_2.

EPR spectroscopy was used to further characterize the heme environment in S160Y. Low-temperature EPR spectra of rsAPX reveals high- and low-spin species (*20*). Consistent with this, the EPR spectrum of S160Y (Figure S1 in the Supporting Information) contains features with a high-spin ferric heme of tetragonal symmetry ($g_\perp = 5.88$, $g_\parallel = 1.99$) and a low-spin species ($g = 2.94$, 2.27, and 1.47). These signals are, however, somewhat different from those observed in the EPR spectrum of rsAPX, which has a high-spin signal with less tetragonality ($g = 5.96$, 5.23, and 1.98), and a less rhombic low-spin signal ($g = 2.68$, 2.21, and 1.78 (*20*)).

In steady-state analyses of S160Y in the presence of ascorbate, the value for k_{cat} ($k_{cat} = 43 \pm 2$ s^{-1}) was lower than that of rsAPX ($k_{cat} = 272 \pm 32$ s^{-1} (*28*)), although K_M values ($K_M = 638 \pm 66$ μM and 389 ± 64 μM (*22*) for S160Y and rsAPX, respectively) were largely similar.

Assessment of Covalent Heme Attachment on Reaction with H_2O_2. Initial experiments indicated that, on reaction with H_2O_2, the heme group in S160Y became covalently attached to the protein. This was tested, qualitatively, in two ways. First, a pyridine hemochromagen assay was carried out before and after reaction with H_2O_2. For S160Y before treatment with H_2O_2, the spectrum of the reduced pyridine hemochromagen complex showed a maximum at 556 nm (Figure 2b). In this experiment, complete extraction of the heme from the protein is observed and the spectrum of the hemochromagen complex is consistent with a noncovalently bound heme structure, in which neither heme vinyl group is modified (*29*). When the same experiment was carried out with S160Y after treatment with 6 equiv of H_2O_2, the peak of the reduced pyridine complex at 556 nm was shifted to 551 nm (Figure 2b). These spectroscopic changes are consistent with covalent modification of the heme vinyl groups (*30*). Second, an acid butanone extraction after reaction of S160Y with H_2O_2 did not remove the heme from the protein, which is a clear indication of covalent attachment of the heme to the protein (Figure S2 in the Supporting Information); in contrast, control experiments with S160Y before reaction with H_2O_2 showed complete extraction of

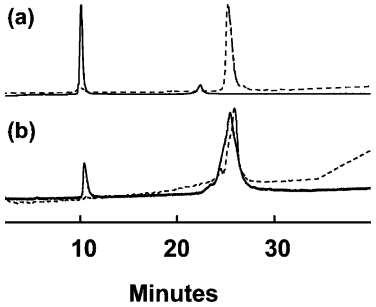

FIGURE 3: HPLC analyses of S160Y before and after reaction with H_2O_2 monitored at 398 nm (solid line) and 215 nm (dotted line). (a) S160Y before reaction with H_2O_2. (b) S160Y after reaction with H_2O_2.

heme into the organic layer. These effects were examined in more detail below.

HPLC Analyses. We sought further confirmation of the proposed heme−protein covalent linkage. HPLC analysis (under denaturing conditions) of the product of the reaction of S160Y with H_2O_2 (prepared with addition of 6 equiv of H_2O_2 as above) showed that the protein (monitored at 215 nm) and the major proportion of the heme (monitored at 398 nm) coelute at 24 min (Figure 3b); a proportion of the protein (≈10%) remains unreacted. This is in direct contrast to the HPLC profile of S160Y which has not been treated with H_2O_2, in which the heme (11 min) and the protein (24 min) do not coelute (Figure 3a). Coelution of the heme and the protein is a clear indication of covalent heme attachment and has been used previously to identify covalently linked heme in various other heme proteins (*3*, *6*, *7*, *11*, *12*, *16*, *31*). A commercial sample of hemin eluted at 11 min, confirming the assignment for free heme above (Figure S3 in the Supporting Information). In separate experiments (data not shown) under the same conditions as those used above for Figure 3b but in the presence of a large excess of ascorbate, it was shown that no peak corresponding to protein-bound heme was observed at ≈24 min. This indicates that under turnover conditions no formation of covalently bound heme occurs.

Mass Spectrometry. Mass spectrometry can be used not only to confirm the presence of a covalent link but also to establish the identity of the residue(s) making the link (*17*). The MALDI-TOF mass spectrum of S160Y before treatment with H_2O_2 showed a mass of 28393.63 Da (Figure 4a), which corresponds closely to the predicted mass (28394.97 Da) of the apoprotein and is consistent with noncovalent attachment of the heme (as found in rsAPX). After treatment with H_2O_2, the main peak in the MALDI-TOF spectrum showed a mass of 29025.68 Da (Figure 4b); this corresponds to an increase in mass of 632 Da over the apoprotein and is consistent with covalent attachment of the heme (616 Da). The additional mass of 16 amu is assigned as arising from hydroxylation of the fragment. Hydroxylation of heme after reaction with H_2O_2 has been reported previously (*11*, *17*).

To establish more clearly the nature of the heme−protein covalent link, tryptic digestion of the product of the reaction of S160Y with H_2O_2 was carried out and HPLC was used to isolate the main heme-containing peptide fragment (i.e., showing both heme and protein absorbances, eluting at 24.7 min, Figure S4 in the Supporting Information) from the resulting peptide mixture. There were three peptide peaks detected on the MALDI-TOF mass spectrum of the main HPLC fragment (Figure 4c). (i) The first peak at 1863.96 Da is the same mass as that observed in identical analyses on rsAPX in which a covalent link to Trp41 has been established (*17*). This peak corresponds to the $L^{39}A\mathbf{W^{41}}$-$HSAGTFDK^{49}$ peptide fragment containing heme covalently bound to Trp41 (*17*). (ii) The second peak at 2971.48 Da is 16 Da higher than the calculated mass (2955.18) expected for the $A^{148}MGLTDQDIVAL\mathbf{Y^{160}}GGHTIGAAHK^{170}$ peptide fragment containing heme covalently bound to Tyr160. (iii) A third peptide fragment was also observed at 4203.39 Da. This is 16 Da higher than the calculated mass (4187.79 Da) expected for the $A^{148}MGLTDQDIVAL\mathbf{Y^{160}}GGHTIGAAHK^{170}$ peptide fragment plus the $L^{39}A\mathbf{W^{41}}HSAGTFDK^{49}$ peptide fragment, with both fragments covalently bound to the heme through Tyr160 and Trp41. The proposed structure of this fragment is shown schematically in the inset to Figure 4d.

MS/MS mass spectrometry was used to obtain more specific sequence information for the third heme-containing fragment at 4203.39 Da. There were two different fragmentation series identified, indicating the presence of two distinct peptides bound to the heme. First, a y-ion fragmentation series allowed sequential identification of His42 through to Thr46 with the remaining C-terminal mass (409.1 Da) consistent with residues Phe47 to Lys49, which corresponds to the sequence $H^{42}SAGTFDK^{49}$ (Figure 4d, series y_B). The absence of fragment ions for the amino acids (LAW^{41}) indicates that the heme forms a covalent link with this part of the peptide and is interpreted as being consistent with the formation of a covalent link toTrp41. This same link has also been shown to form when rsAPX is reacted with H_2O_2 (*17*). Second, a separate y-ion fragmentation series allowed sequential identification of His163 through to Lys170, which corresponds to the sequence $H^{163}TIGAAHK^{170}$ (Figure 4d, series y_A). A combination of a- and b-ion fragmentation series allowed sequential identification of Ala148 through to Asp152, which corresponds to the sequence $A^{148}MGLTD^{152}$ on the N-terminal end of this peptide (Figure 4d, series a/b_A). As above, the absence of fragment ions for the amino acids ($QDIVAL\mathbf{Y^{160}}GG$) indicates that the heme forms a covalent link with this part of the peptide (in Figure 4d, inset).

Further evidence for heme incorporation into the peptides mentioned above came from isotope patterns of the peptides in question. Because iron exhibits a very distinct isotope pattern, when incorporated into protoporphyrin IX to form heme it produces very characteristic signals. Figure 5a, left, shows the theoretical isotope pattern of heme, and Figure 5a, right, shows the isotope pattern obtained from MALDI-TOF mass spectrometry of heme. Theoretical isotope patterns were also calculated for the two heme-free peptides containing Trp41 ($L^{39}A\mathbf{W^{41}}HSAGTFDK^{49}$, Figure 5b, left) and Tyr160 ($A^{148}MGLTDQDIVAL\mathbf{Y^{160}}GGHTIGAAHK^{170}$, Figure 5d, left) and were in very good agreement with the experimental isotope patterns obtained for these peptides (Figures 5b, 5d, right). The same procedure was used to calculate theoretical isotope patterns for the same peptide fragments but with heme covalently attached (i.e., after treatment with H_2O_2). Hence, the peptide fragment with a mass of 1864 Da (Figure 4c) was assigned above to the fragment $L^{39}A\mathbf{W^{41}}HSAGTFDK^{49}$ with heme covalently bound: this peptide exhibits the same characteristic isotope pattern (Figure 5c, right) as that predicted theoretically after

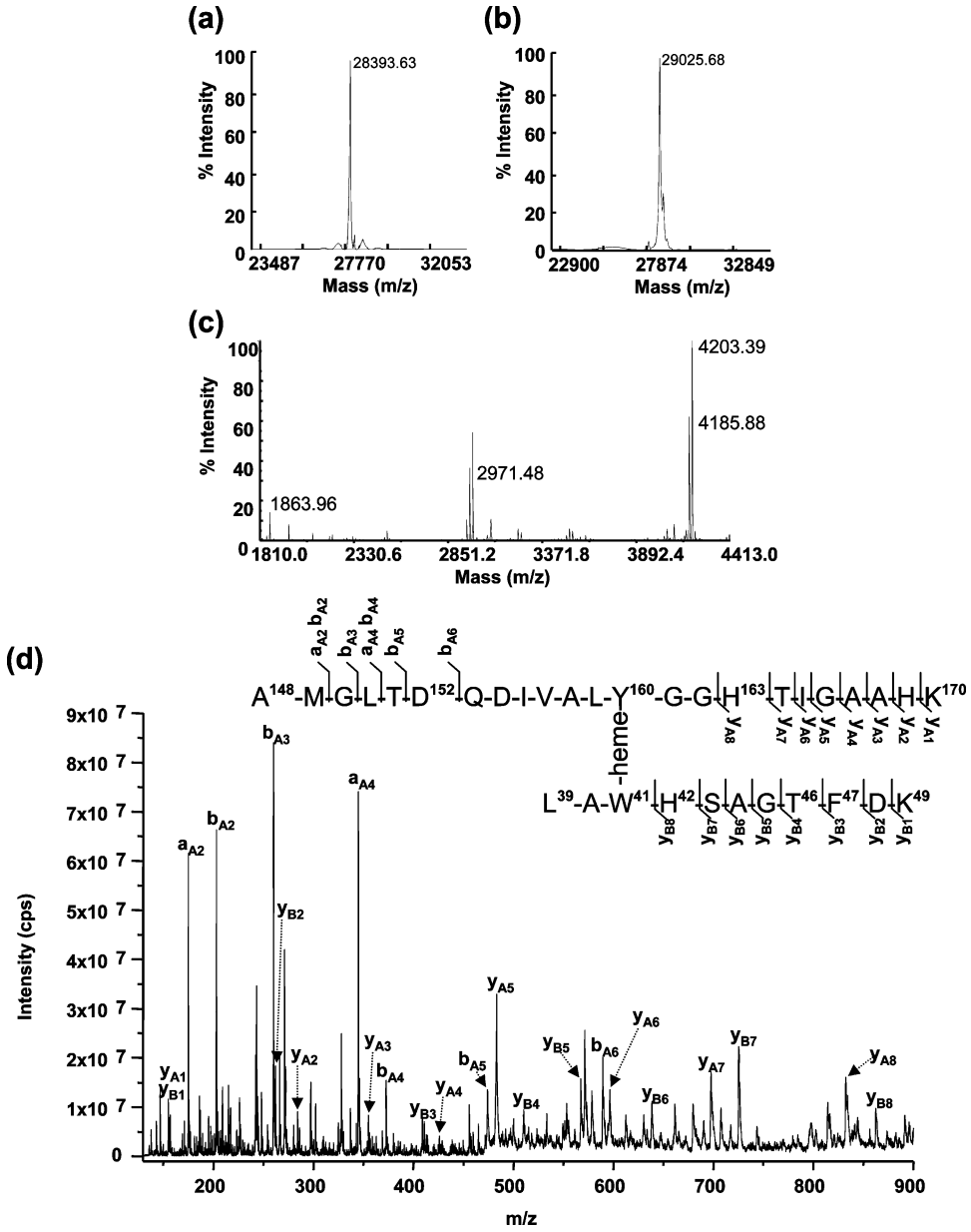

FIGURE 4: MALDI-TOF mass spectrum of S160Y before (a) and after (b) reaction with 6 equiv of H_2O_2. (c) MALDI-TOF mass spectrum of the HPLC-purified heme-containing peptide fragment obtained after reaction of S160Y with H_2O_2. (d) MS/MS spectrum of the HPLC-purified heme-containing peptide fragment showing the 4+ charged precursor ion (1051.44 Da). The peptide sequences obtained correspond to the y-ion fragment series for LA**W**^{41}HSAGTFDK peptide and the a-, b-, and y-ion fragment series for the AMGLTDQDIVAL**Y**^{160}-GGHTIGAAHK peptide and are shown (inset).

attachment of heme (Figure 5c, left) which confirms the assignment. Similarly, the same change in isotope pattern is observed for the peptide with a mass of 2971 Da (Figure 4c), assigned above as A^{148}MGLTDQDIVAL**Y**^{160}-GGHTIGAAHK^{170} with heme covalently attached, before and after attachment of heme, Figures 5d and 5e. The fact that the peptides with masses of 1864 Da (Figure 5c) and 2971 Da (Figure 5e) exhibit the same characteristic isotope pattern as heme (Figure 5a) gives further confirmation of their assignment as heme-containing peptides.

Mechanistic Investigations. Reaction of ferric S160Y with 6 equiv of H_2O_2 was monitored over ~2 h, and the intermediate spectra are presented in Figure 6a. In contrast to the wild type protein in which a Compound I species (containing a porphyrin π-cation radical) is clearly visible on the stopped-flow time scale and a Compound II species is clearly visible on a time scale of 1−2 min (*28*), reaction of S160Y with H_2O_2 did not show any evidence for formation of either Compound I or Compound II using conventional electronic spectroscopy. Instead, the reaction resulted in a final product with wavelength maxima at 408, 530, and 563 nm (Figure 6a).

The same reaction was also examined under pre-steady-state conditions (Figure 6b), to investigate if reaction of S160Y with H_2O_2 involved initial formation of a Compound I intermediate over shorter time scales (300 ms to 4200 s) and using different H_2O_2 concentrations (6 to 100 equiv). Unlike rsAPX which shows clear formation of a Compound I intermediate containing a porphyrin π-cation radical (λ_{max}/nm = 409, 530, 569^{sh}, and 655 (*17*)) on reaction with H_2O_2 under rapid mixing conditions, no formation of a porphyrin π-cation radical intermediate was observed under any condi-

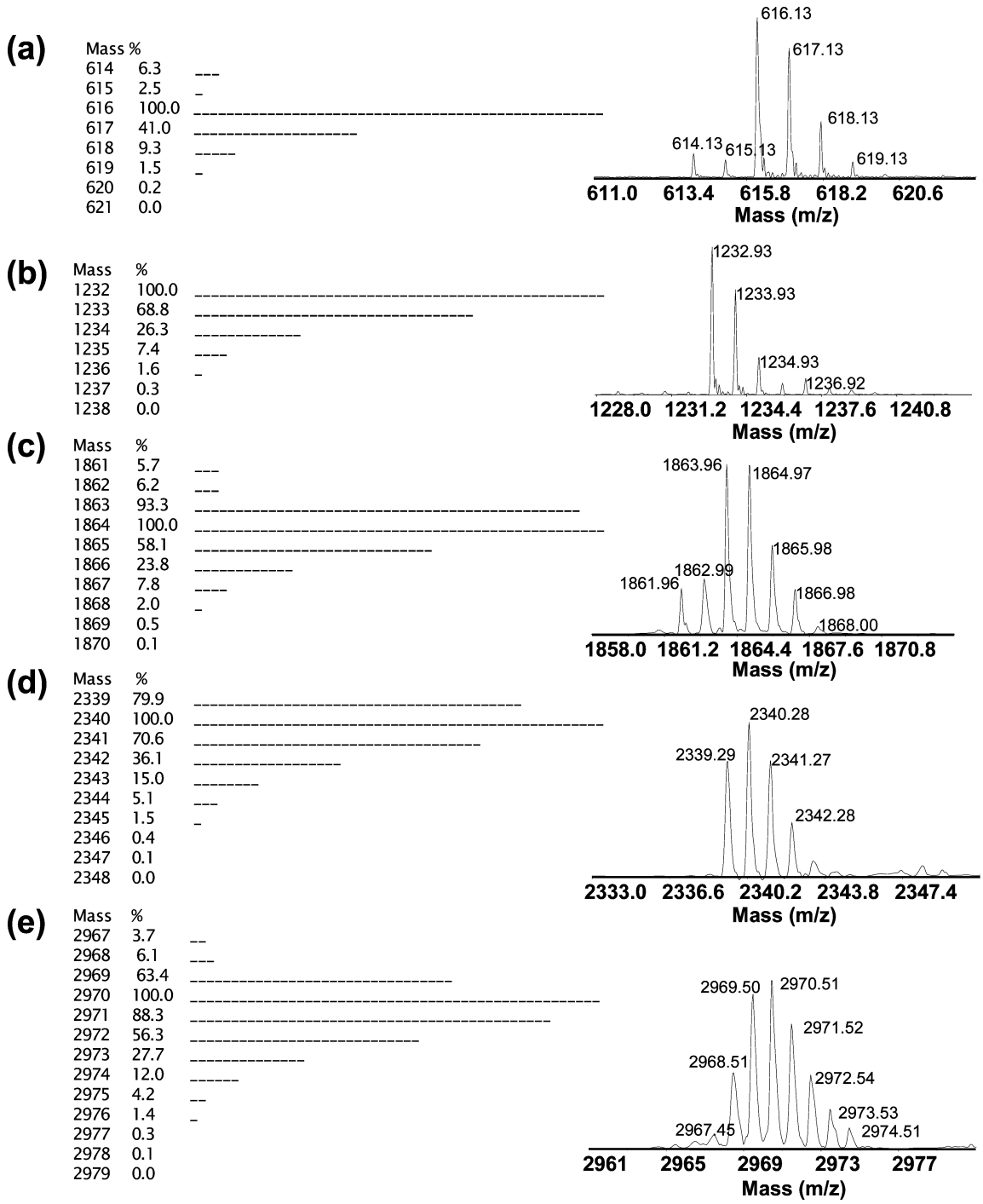

FIGURE 5: Theoretically calculated (figures on the left) and experimentally observed (figures on the right) isotope patterns for heme (a), the LA**W**^{41}HSAGTFDK peptide before (b) and after (c) covalent attachment of heme, and the AMGLTDQDIVAL**Y**^{160}GGHTIGAAHK peptide before (d) and after (e) covalent attachment of heme.

tions for S160Y. (Over time scales <300 ms and >1.28 ms (the dead-time of the stopped-flow instrument), no formation of a porphyrin π-cation radical intermediate was observed either.) Instead, on reaction of S160Y with H_2O_2 the Soret peak is blue-shifted and decays to a final spectrum with maxima (408, 530, and 563 nm) similar to those described above (Figure 6a). Time-dependent spectra were fitted globally by numerical integration methods using Prokin software (Applied Photophysics). Data collected over a period of 1000 s from the mixing event were best fitted to a two-step model (A $\rightarrow$ B $\rightarrow$ C, with rate constants for these two steps of 0.028 s^{-1} and 0.0024 s^{-1}, respectively) (Figure 6c). Intermediate A has absorption characteristics (λ_{max}/nm = 413, 529, and 562$^{(sh)}$ nm) consistent with those observed above for ferric S160Y, and clearly arise from the oxidized enzyme. Intermediate B (λ_{max}/nm = 411, 528, and 558$^{(sh)}$ nm) does not show spectroscopic characteristics that are consistent with either Compound I or Compound II. Intermediate C has maxima that are consistent with the final product of the reaction of S160Y with H_2O_2 (Figure 6a). These findings show that exposure of the protein to H_2O_2 does not lead to formation of the expected porphyrin π-cation radical, which is in contrast to rsAPX and all other APXs examined so far (*32*). They also indicate that the formation

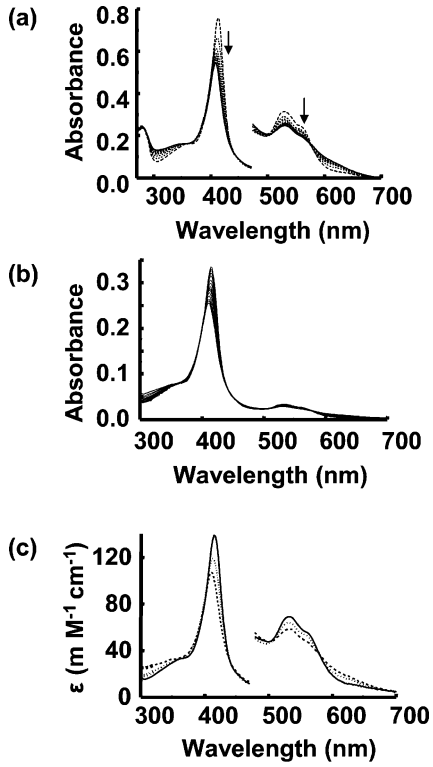

FIGURE 6: (a) Selected spectra collected during the reaction of ferric S160Y (dashed line) with 6 equiv of H_2O_2. Intermediate spectra between ferric S160Y and the final product (solid line) are shown as dotted lines. The total reaction time was 2 h. The visible region has been multiplied by a factor of 5. Sample conditions: enzyme 5 μM, hydrogen peroxide 30 μM, 0.1 M potassium phosphate, pH 7.0, 25.0 °C. (b) Reaction of S160Y with H_2O_2 monitored by stopped-flow diode array spectroscopy. Conditions: 100 mM potassium phosphate buffer, pH 7.0; 25 °C. Enzyme concentration, 20 μM; substrate concentration, 30 mM. The experiment is performed over 1000 s. For clarity, only selected spectra are shown. (c) Deconvoluted spectra for the reaction shown in (b). The data were fitted to a two-step model: intermediate A shown in solid line, intermediate B shown in dotted line, and intermediate C shown in dashed line.

of these links is slower overall than that observed for formation of other cross-links in APX which are known to go through formation of an authentic porphyrin π-cation intermediate (*11*).

Electron Paramagnetic Resonance. EPR spectroscopy was used to obtain further evidence for the formation of a protein radical. EPR spectra of rsAPX and S160Y after treatment with H_2O_2 are shown in Figure 7a and 7b, respectively. In agreement with previous work (*33*), reaction of rsAPX with H_2O_2 yields a species with *g*-values ($g = 3.52$, $g = 1.998$) consistent with the existence of a porphyrin π-cation radical (Figure 7a). In contrast, reaction of S160Y with H_2O_2 (Figure 7b) reveals a single radical species with $g = 2.0053$ and a line width of 19.2 G. This signal is shown in more detail in Figure 7c and is compared with the EPR signal (Figure 7d) observed in the human metHb/H_2O_2 system in which a tyrosyl radical has been assigned (*34*). These EPR signals, Figures 7c and 7d, have identical *g*-factors and linewidths and have very close overall lineshapes. The maximal yield of the free radical, observed at the first time points of the reaction (4−10 s), was 0.3 μM for the stoichiometric amount of H_2O_2 added and 0.5 μM for a 6-fold molar excess of H_2O_2 over the heme concentration (80 μM). A low concentration

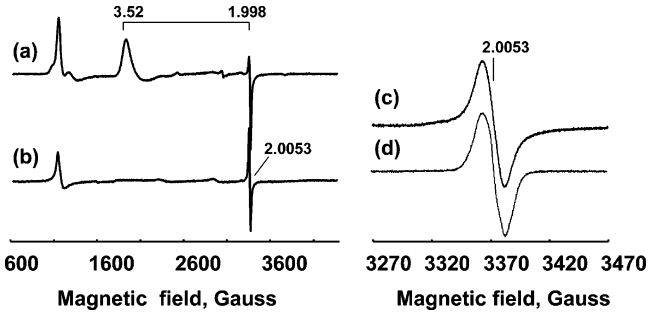

FIGURE 7: The EPR spectra of (a) rsAPX and (b) S160Y (both 80 μM) after addition of 80 μM H_2O_2 (final concentrations, pH 7.0, the samples frozen 4 s after mixture). The spectra were measured at 10 K; other instrumental conditions were modulation frequency $\nu_m = 100$ kHz, modulation amplitude $A_m = 5$ G, sweep rate $\upsilon = 22.6$ G/s, time constant $\tau = 82$ ms, microwave frequency $\nu = 9.47$ GHz, microwave power $P = 3.188$ mW, number of spectral scans NS = 1. (c) Detailed EPR spectrum of the free radical formed in S160Y after addition of H_2O_2; sample conditions as in (b), instrumental conditions were as in (b) except $A_m = 3$ G and $\upsilon = 1.19$ G/s. (d) A tyrosyl radical EPR signal recorded under the same conditions as (c) in the human metHb + H_2O_2 system (*34*).

of free radicals observed (under 1% of protein) is in agreement with previous reports on different heme protein/peroxide systems (*34*, *35*). Taken together, these data are consistent with the stopped-flow data presented above and are consistent with the formation of a tyrosyl radical.[2] Power saturation studies (data not shown) revealed that the radical in the S106Y mutant relaxed faster than many radicals observed so far on proteins, which suggests proximity to a nearby paramagnetic center, consistent with its presence on the Tyr160 and close to the heme.

Redox Measurements. The Fe^{3+}/Fe^{2+} reduction potential for S160Y before reaction with H_2O_2 (determined using the phenosafranine/xanthine/xanthine oxidase method) was found to be −197 mV, Figure 8a; this compares with a value of −206 mV (*25*) for rsAPX and indicates that no considerable shift in potential occurred as a consequence of the S160Y mutation. The corresponding Fe^{3+}/Fe^{2+} reduction potential for S160Y after reaction with H_2O_2 was determined using indigo trisulfonate as a dye (Figure 8b) and was found to be −98 mV, an increase of 99 mV. Both sets of data show linear Nernst plots, Figure 8c. This suggests that the formation of two covalent links between the heme and the protein in S160Y leads to a significant stabilization of the reduced protein.

DISCUSSION

The heme prosthetic group is widely distributed in biological systems and in the majority of cases is bound to the protein through noncovalent interactions. There are still relatively few examples of heme proteins or enzymes in which the heme substituents (i.e., the vinyl and/or methyl groups) are covalently bound to the protein backbone (*1*, *2*, *8*, *9*, *36*−38). For many years, therefore, the prevailing view was that the substituents on the heme group were inherently unreactive and that formation of these links could only be supported within a very specific and highly tuned structural

[2] We note that no such radical is observed before introduction of Tyr at position 160. However, the possibility that the radical might be at a different location to Tyr160 cannot be ruled out.

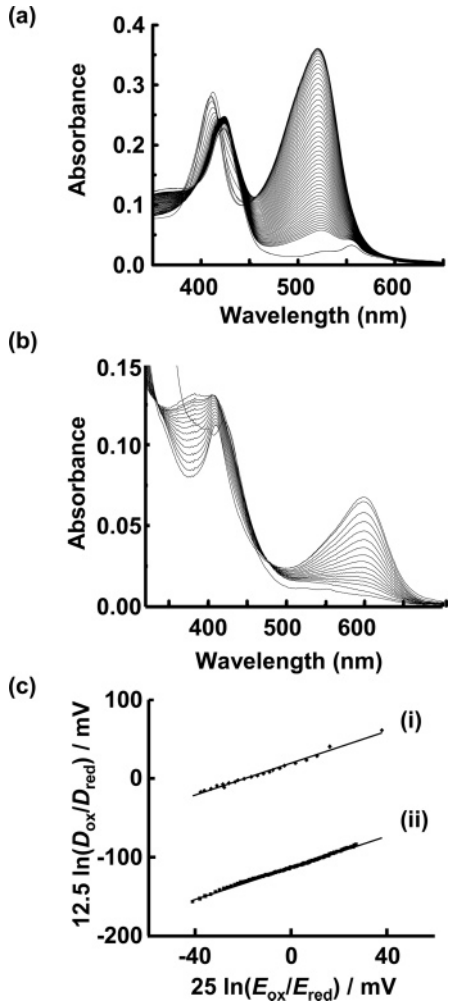

FIGURE 8: Representative family of spectra for determination of Fe^{3+}/Fe^{2+} reduction potential in S160Y before (a) and after (b) reaction with H_2O_2 (100 mM potassium phosphate, pH 7.0). (c) The corresponding linear Nernst plots, where plot (i) corresponds to the data shown in (b) and plot (ii) to the data shown in (a).

and/or catalytic framework. This simplistic rationalization now appears to represent only one part of a much more sophisticated problem. Hence, *in vitro* studies from different laboratories (*11*−*16*) have revealed that most of these covalent links can be duplicated in other protein architectures when the correct residue is introduced in the correct place and if the correct oxidation states of the metal are accessible. This is supported by other examples in which covalent links to various heme proteins have also been observed without needing to introduce specific mutations in the active site (*17*, *31*, *39*−*41*).

This paper provides further evidence in support of the above hypothesis. Hence, we have already shown (*11*) that replacement of Ser160 in ascorbate peroxidase by a methionine residue leads to formation of a heme−methionine covalent link in an autocatalytic reaction that requires H_2O_2. Here, we establish that the introduction of a nucleophilic tyrosine residue at this position leads, similarly, to a covalent link to Tyr160. In addition, a second covalent link to Trp41 is observed: this link has been previously shown (*17*) to form to the 4-vinyl group of the heme in the wild type protein through an autocatalytic reaction involving reaction with H_2O_2. To our knowledge, there is only one other example (*15*) in which formation of a doubly linked heme species has been engineered inside a protein architecture that does not, ordinarily, support such links.

The Nature of the Tyrosine−*Heme Link.* Based on our previous work in which a covalent link from Met160 to the 2-vinyl was proposed, we had originally envisaged a similarly modified heme for the S160Y variant. The peak at 551 nm for the reduced pyridine−heme complex of S160Y after treatment with H_2O_2 has been used as an empirical indication that two vinyl groups on the porphyrin ring have been modified (*29*): since we had already established that Trp41 links to the 4-vinyl group (*17*), the 551 nm peak indicated that Tyr160 was linked to the 2-vinyl group. There are only a handful of examples in the literature of tyrosine−heme covalent links: in the cytochrome P460 heme in hydroxylamine oxidoreductase (HAO) (*36*, *42*), in myoglobin (*39*), and in leghemoglobin (*40*). In all three cases, the link has been proposed to a *meso*-carbon of the heme (although not the same *meso*-carbon in all cases), but this has not been confirmed crystallographically. There is, however, a structure for the cytochrome P460 from *Nitrosomonas europaea* (*37*) in which a covalent link from the γ-meso carbon of the heme to the amine group of a lysine residue has been observed. By analogy, it has been proposed (*37*) that the heme−tyrosine link in HAO is to the hydroxyl group of the Tyr residue and that the heme−tyrosine (in HAO) and heme−lysine (in P460 from *Nitrosomonas europaea*) links are formed either through a radical mechanism or by direct nucleophilic attack. From the data presented above for S160Y, we cannot confirm unambiguously the precise nature of the heme−tyrosine link, but analogy with the examples above would suggest that a link to the *meso*-carbon is most likely. This would be consistent with our control experiments and parallel HPLC analyses with apo-S160Y reconstituted with deuteroheme (in which hydrogen atoms replace the 2- and 4-vinyl groups) in which we observed that replacement of the heme vinyl groups reduced the percentage of covalently linked heme but did not eliminate it completely (Figure S4 in the Supporting Information[3]).

The Mechanism of Formation of the Links. Stopped-flow data shows no evidence for formation of a typical Compound I species (containing a porphyrin π-cation radical) on reaction of S160Y with H_2O_2. EPR experiments similarly showed no evidence for formation of a porphyrin π-cation signal as observed for the wild type enzyme (*33*); instead, EPR identifies an initial radical species which was assigned as a tyrosyl radical. This is shown as Intermediate I in Scheme 1, in which we outline a proposed mechanism for formation of the covalent links to the heme. This initially formed species may arise in two ways: (a) indirectly, through internal electron transfer within an initial porphyrin π-cation species that is not observable on the stopped-flow time scale (steps (i) and (ii), Scheme 1); or (b) directly through oxidation of Tyr160 on reaction with H_2O_2 (step (iii) in Scheme 1), without going through a normal Compound I intermediate. There is separate evidence that formation of

[3] We estimate that the percentage formation of total covalently linked product reduces by ≈20% for deuteroheme (from ≈90% for S160Y + iron protoporphyrin IX + H_2O_2), and we assume that the link is to the meso-carbon for this deuteroheme species (since the vinyl groups are missing). In these experiments, our methods of separation for these modified fragments are not sensitive enough to pick up minor cross-linked components if they were present.

Scheme 1: Proposed Mechanism for Formation of a Covalent Link between Tyr160 and the Heme in Ascorbate Peroxidase[a]

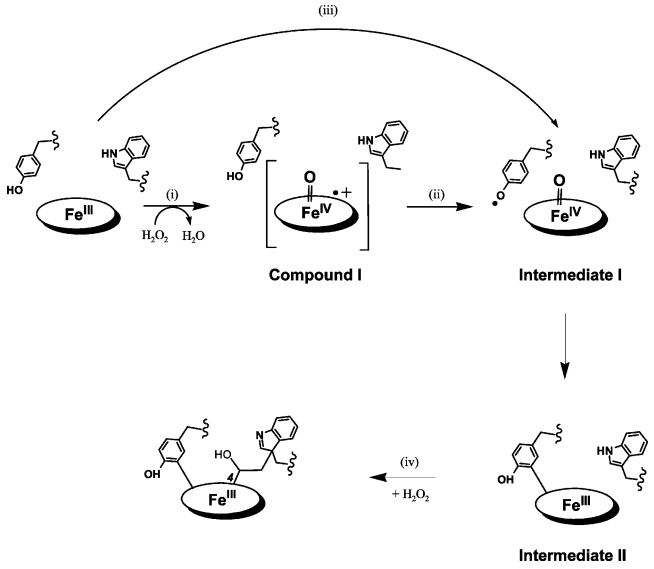

[a] The heme−Trp link, step (iv), is at the 4-vinyl group (labeled with a 4 in the scheme) with a suggested structure (*17*) as shown; this is proposed to be via formation of a Trp radical and to be through the C^{γ} of Trp41, but the various resonance forms of a Trp radical mean that a link to other carbon atoms of Trp41 is also possible. The structure of the heme−Tyr link is not known and is suggested to be as depicted here; an ether link through the O of Tyr160 is also possible, however. The porphyrin π-cation radical is not detected in this work, but is proposed as an intermediate on the basis of the known mechanism in the wild type enzyme (see Discussion).

tyrosyl radicals can occur independently and not necessarily as a consequence of Compound I formation (*43*). We cannot distinguish these two possibilities from the data presented. We then envisage a further radical reaction mechanism to form the heme−tyrosine link, Scheme 1, followed by further reaction with H_2O_2 to form the heme−Trp link, step (iv) in Scheme 1. We have proposed (*17*) that formation of this link to Trp41 involves radical formation on Trp41.

Functional Implications. We have observed that formation of a double link between the heme and Tyr160 and Trp41 resulted in an increase of the Fe^{3+}/Fe^{2+} reduction potential from −197 mV to −98 mV, reflecting a clear stabilization of the reduced form. Parallel experiments with rsAPX after formation of the Trp41−heme linkage also showed an increase in the Fe^{3+}/Fe^{2+} reduction potential (data not shown) although this increase was difficult to quantify because of the experimental complications associated with obtaining completely pure samples of the Trp41−heme species. Hence, we cannot assign the 99 mV stabilization of the reduced form in the modified enzyme as arising from one or other of the two links, although we note also that covalent modification of the flavin (FAD) subunit of the flavocytochrome *p*-cresol methylhydroxylase by a Tyr residue also raises the reduction potential of the flavin group (*44*). In fact, quantitative rationalizations of the role of individual covalent links on the control of heme redox potential are very poorly defined. The closest analogy is with the mammalian peroxidases, in which the covalent links to the heme have been linked with their redox properties. Although there is no overall consensus on exactly how and why these links are influential, disruption of the Asp94−heme ester linkage in myeloperoxidase has been shown to lead to changes in heme potential, suggested to be a result of increased heme flexibility introduced as a consequence of the removal of one of the three physiological covalent links (*45*). It is possible that similar effects on the heme structure are responsible for the changes we observe in this work.

ACKNOWLEDGMENT

This paper is dedicated to the memory of Professor Geoff Sykes.

NOTE ADDED AFTER ASAP PUBLICATION

This paper was published ASAP on October 25, 2007 with an error in the Abstract. The correct version published on November 13, 2007.

SUPPORTING INFORMATION AVAILABLE

The EPR spectrum of ferric S160Y (Figure S1), acid butanone extraction for S160Y (Figure S2), HPLC analysis for free heme (Figure S3), HPLC of tryptic digest of S160Y after reaction with H_2O_2 (Figure S4), and HPLC analyses of S160Y reconstituted with deuteroheme (Figure S5). This material is available free of charge via the Internet at http://pubs.acs.org.

REFERENCES

1. Stevens, J. M., Daltrop, O., Allen, J. W. A., and Ferguson, S. J. (2004) *C*-type cytochrome formation: chemical and biological enigmas, *Acc. Chem. Res. 37*, 999−1007.
2. Colas, C., and Ortiz de Montellano, P. R. (2003) Autocatalytic radical reactions in physiological prosthetic heme modification, *Chem. Rev. 103*, 2305−2332.
3. Colas, C., Kuo, J. M., and Ortiz de Montellano, P. R. (2002) Asp-225 and Glu-375 in autocatalytic attachment of the prosthetic heme group of lactoperoxidase, *J. Biol. Chem. 277*, 7191−7200.
4. Rae, T. D., and Goff, H. M. (1998) The heme prosthetic group of lactoperoxidase. Structural characteristics of heme l and heme l-peptides, *J. Biol. Chem. 273*, 27968−27977.
5. Oxvig, C., Thomsen, A. R., Overgaard, M. T., Sorensen, E. S., Hojrup, P., Bjerrum, M. J., Gleich, G. J., and Sottrup-Jensen, L. (1999) Biochemical evidence for heme linkage through esters with Asp-93 and Glu-241 in human eosinophil peroxidase. The ester with Asp-93 is only partially formed in vivo, *J. Biol. Chem. 274*, 16953−16958.
6. LeBrun, L. A., Xu, F., Kroetz, D. L., and Ortiz de Montellano, P. R. (2002) Covalent attachment of the heme prosthetic group in the CYP4 cytochrome P450 family, *Biochemistry 41*, 5931−5937.
7. Henne, K. R., Kunze, K. L., Zheng, Y.-M., Christmas, P., Soberman, R. J., and Rettie, A. E. (2001) Covalent linkage of prosthetic heme to CYP4 family of P450 enzymes, *Biochemistry 40*, 12925−12931.
8. Hoy, J. A., Kundu, S., Trent, J. T., III, Ramaswamy, S., and Hargrove, M. S. (2004) The crystal structure of *Synechocystis* hemoglobin with a covalent heme linkage, *J. Biol. Chem. 279*, 16535−16542.
9. Lee, D., Pervushin, K., Dischof, D., Braun, M., and Thony-Meyer, L. (2005) Unusual heme-histidine bond in the active site of a chaperone, *J. Am. Chem. Soc. 127*, 3716−3717.
10. Uchida, T., Stevens, J. M., Daltrop, O., Harvat, E. M., Hong, L., Ferguson, S. J., and Kitagawa, T. (2004) The interaction of covalently bound heme with the cytochrome *c* maturation protein CcmE, *J. Biol. Chem. 279*, 51981−51988.
11. Metcalfe, C. L., Ott, M., Patel, N., Singh, K., Mistry, S. C., Goff, H. M., and Raven, E. L. (2004) Autocatalytic formation of green heme: evidence for H_2O_2-dependent formation of a covalent methionine-heme linkage in ascorbate peroxidase, *J. Am. Chem. Soc. 126*, 16242−16248.
12. Colas, C., and De Montellano, P. R. (2004) Horseradish peroxidase mutants that autocatalytically modify their prosthetic heme

group: insights into mammalian peroxidase heme-protein covalent bonds, *J. Biol. Chem. 279*, 24131−24140.
13. Huang, L., Wojciechowski, G., and Ortiz de Montellano, P. R. (2006) Role of heme-protein covalent bonds in mammalian peroxidases. Protection of the heme by a single engineered heme-protein link in horseradish peroxidase, *J. Biol. Chem. 281*, 18983−18988.
14. Barker, P. D., Ferrer, J. C., Mylrajan, M., Loehr, T. M., Feng, R., Konishi, Y., Funk, W. D., MacGillivray, R. T., and Mauk, A. G. (1993) Transmutation of a heme protein, *Proc. Natl. Acad. Sci. U.S.A. 90*, 6542−6546.
15. Barker, P. D., Nerou, E. P., Freund, S. M., and Fearnley, I. M. (1995) Conversion of cytochrome b562 to c-type cytochromes, *Biochemistry 34*, 15191−15203.
16. Limburg, J., LeBrun, L. A., and Ortiz de Montellano, P. R. (2005) The P450cam G248E mutant covalently binds its prosthetic heme group, *Biochemistry 44*, 4091−4099.
17. Pipirou, Z., Bottrill, A. R., Metcalfe, C. M., Mistry, S. C., Badyal, S. K., Rawlings, B. J., and Raven, E. L. (2007) Autocatalytic Formation of a Covalent Link between Tryptophan 41 and the Heme in Ascorbate Peroxidase, *Biochemistry 46*, 2174−2180.
18. Nelson, D. P., and Kiesow, L. A. (1972) Enthalpy of decomposition of hydrogen peroxide by catalase at 25 degrees C (with molar extinction coefficients of H_2O_2 solutions in the UV), *Anal. Biochem. 49*, 474−478.
19. Badyal, S. K., Joyce, M. G., Sharp, K. H., Seward, H. E., Mewies, M., Basran, J., Macdonald, I. K., Moody, P. C. E., and Raven, E. L. (2006) Conformational mobility in the active site of a heme peroxidase, *J. Biol. Chem. 281*, 24512−24520.
20. Jones, D. K., Dalton, D. A., Rosell, F. I., and Lloyd Raven, E. (1998) Class I heme peroxidases: characterisation of soybean ascorbate peroxidase, *Arch. Biochem. Biophys. 360*, 173−178.
21. Teale, F. W. J. (1959) Cleavage of the haem-protein link by acid methylethylketone, *Biochim. Biophys. Acta 35*, 543.
22. Lad, L., Mewies, M., and Raven, E. L. (2002) Substrate binding and catalytic mechanism in ascorbate peroxidase: evidence for two ascorbate binding sites, *Biochemistry 41*, 13774−13781.
23. Weil, J. A., Bolton, J. R., and Wertz, J. E. (1994) *Electron paramagnetic resonance: Elementary theory and practical applications*, p xxi, Wiley, New York.
24. Massey, V. (1991) in *Flavins and Flavoproteins* (Curti, B., Ronchi, S., and Zanetti, G., Eds.) pp 59−66, Walter de Gruyter & Co., New York.
25. Efimov, I., Papadopoulou, N. D., McLean, K. J., Badyal, S. K., Macdonald, I. K., Munro, A. W., Moody, P. C., and Raven, E. L. (2007) The Redox Properties of Ascorbate Peroxidase, *Biochemistry 46*, 8017−8023.
26. Clark, W. M. (1972) *Oxidation-Reduction Potentials of Organic Systems*, Robert E. Kreiger Publishing Co., Huntington, NY.
27. Binstead, R. A., and Zuberbuehler, A. D., Chapel Hill, NC.
28. Lad, L., Mewies, M., and Raven, E. L. (2002) Substrate binding and catalytic mechanism in ascorbate peroxidase: evidence for two ascorbate binding sites, *Biochemistry 41*, 13774−13781.
29. Antonini, M., and Brunori, E. (1971) *Hemoglobin and Myoglobin and their reactions with ligands*, North Holland Publishers, Amsterdam.
30. Daltrop, O., Smith, K. M., and Ferguson, S. J. (2003) Stereoselective *in vitro* formation of *c*-type cytochrome variants from *Hydrogenobacter thermophilus* containing only a single thioether bond, *J. Biol. Chem. 278*, 24308−24313.
31. Reeder, B. J., Svistunenko, D. A., Sharpe, M. A., and Wilson, M. T. (2002) Characteristics and mechanism of formation of peroxide-induced heme to protein cross-linking in myoglobin, *Biochemistry 41*, 367−75.
32. Raven, E. L. (2003) Understanding functional diversity and substrate specificity in haem peroxidases: what can we learn from ascorbate peroxidase, *Nat. Prod. Rep. 20*, 367−381.
33. Patterson, W. R., Poulos, T. L., and Goodin, D. B. (1995) Identification of a porphyrin pi cation radical in ascorbate peroxidase compound I, *Biochemistry 34*, 4342−4345.
34. Svistunenko, D. A., Dunne, J., Fryer, M., Nicholls, P., Reeder, B. J., Wilson, M. T., Bigotti, M. G., Cutruzzola, F., and Cooper, C. E. (2002) Comparative study of tyrosine radicals in hemoglobin and myoglobins treated with hydrogen peroxide, *Biophys. J. 83*, 2845−285.
35. Svistunenko, D. A. (2005) Reaction of haem containing proteins and enzymes with hydroperoxides: the radical view, *Biochim. Biophys. Acta 1707*, 127−155.
36. Arciero, D. M., Hooper, A. B., Cai, M., and Timkovich, R. (1993) Evidence for the structure of the active site heme P460 in hydroxylamine oxidoreductase of Nitrosomonas, *Biochemistry 32*, 9370−9378.
37. Pearson, A. R., Elmore, B. O., Yang, C., Ferrara, J. D., Hooper, A. B., and Wilmot, C. M. (2007) The Crystal Structure of Cytochrome P460 of Nitrosomonas europaea Reveals a Novel Cytochrome Fold and Heme-Protein Cross-link, *Biochemistry 46*, 8340−8349.
38. Vu, B. C., Vuletich, D. A., Kuriakose, S. A., Falzone, C. J., and Lecomte, J. T. (2004) Characterization of the heme-histidine cross-link in cyanobacterial hemoglobins from Synechocystis sp. PCC 6803 and Synechococcus sp. PCC 7002, *J. Biol. Inorg. Chem. 9*, 183−194.
39. Catalano, C. E., Choe, Y. S., and Ortiz de Montellano, P. R. (1989) Reactions of the protein radical in peroxide-treated myoglobin. Formation of a heme-protein cross-link, *J. Biol. Chem. 264*, 10534−10541.
40. Moreau, S., Davies, M. J., and Puppo, A. (1995) Reaction of ferric leghemoglobin with H_2O_2: formation of heme-protein cross-links and dimeric species, *Biochim. Biophys. Acta 1251*, 17−22.
41. Jia, Y., Buehler, P. W., Boykins, R. A., Venable, R. M., and Alayash, A. I. (2007) Structural basis of peroxide-mediated changes in human hemoglobin: a novel oxidative pathway, *J. Biol. Chem. 282*, 4894−4907.
42. Igarashi, N., Moriyama, H., Fujiwara, T., Fukumori, Y., and Tanaka, N. (1997) The 2.8 A structure of a hydroxylamine oxidoreductase from a denitrifying chemoautotrophic bacterium, *Nitrosomonas europaea*, *Nat. Struct. Biol. 4*, 276−284.
43. Zhang, H., He, S., and Mauk, A. G. (2002) Radical formation at Tyr39 and Tyr153 following reaction of yeast cytochrome *c* peroxidase with hydrogen peroxide, *Biochemistry 41*, 13507−13513.
44. Efimov, I., Cronin, C. N., and McIntire, W. S. (2001) Effects of noncovalent and covalent FAD binding on the redox and catalytic properties of p-cresol methylhydroxylase, *Biochemistry 40*, 2155−2166.
45. Zederbauer, M., Furtmuller, P. G., Bellei, M., Stampler, J., Jakopitsch, C., Battistuzzi, G., Moguilevsky, N., and Obinger, C. (2007) Disruption of the aspartate to heme ester linkage in human myeloperoxidase: impact on ligand binding, redox chemistry, and interconversion of redox intermediates, *J. Biol. Chem. 282*, 17041−17052.

BI7015316